

A Multispecies Traffic Model based on the Lighthill-Whitham Richards Model

Rinaldo M. Colombo, Christian Klingenberg and Marie-Christine Meltzer

Abstract We consider an extension of the macroscopic traffic model of Lighthill- Whitham and Richards to a multispecies traffic model. As has already been observed by Benzoni-Gavage and Colombo [2003] the system of PDEs lacks strict hyperbolicity. We study the Riemann Problem for the two species extension with focus on the values around the umbilic point, where the eigenvalues coalesce. For this purpose, we examine the behavior of the solutions around the critical point like it is done by Meltzer [2016]. Due to the difficulty of the umbilic point, we are not able to prove well posedness analytically. But we provide an understanding of the systems properties via numerical experiments which leads to the conjecture, that the Riemann Problem has a unique solution on the whole set of definition.

1 Introduction

In this paper we consider a macroscopic traffic model which means that we assume a large number of vehicles on the road and describe them through their density. A famous and well studied model describing the traffic density and its evolution, is the model of Lighthill-Whitham and Richards (LWR). It is deduced assuming the conservation of vehicles and that their speed depends solely on their density. The wish to discriminate different types of vehicles, like for example cars and trucks, leads to the consideration of a multi species extension of this model that has already been proposed in literature. This extension leads to difficulties in proving well posedness already for two species, since it contains an umbilic point where the system is not hyperbolic and hence we are not able to use the standard theory for hyperbolic systems. In this paper, the solution to the Riemann problem is studied around the critical point to see how the lack of hyperbolicity affects the solutions.

First of all, we introduce the LWR Model, its variables and the Greenshields velocity function which was first studied by Lighthill and Whitham [1955] and Richards [1956]. From the macroscopic point of view, there are three fundamental variables describing car traffic. As a first step, we consider a one-lane road where all traffic participants are of one species and overtaking is forbidden. Then, we describe the

Rinaldo M. Colombo
INdAM Unit
Brescia University, Via Valotti 9, 25133 Brescia, Italy
e-mail: rinaldo.colombo@unibs.it

Christian Klingenberg
Dept. of Mathematics at Würzburg University
Emil Fischer Str. 40, Würzburg, 97074, Germany
e-mail: klingen@mathematik.uni-wuerzburg.de

Marie-Christine Meltzer
Dept. of Mathematics at Würzburg University
Emil Fischer Str. 40, Würzburg, 97074, Germany
e-mail: marie.meltzer@hotmail.de

velocity, the density and the traffic flow as functions of the space coordinate $x \in \mathbb{R}$ and of time $t \in \mathbb{R}^+$. The velocity of cars is described by the velocity field u and the traffic density ρ measures the number of vehicles per unit length of the road. Alternatively, ρ can be viewed as the occupancy, i.e., as the fraction of road length occupied by vehicles. Finally, the traffic flow f is the third macroscopic variable, defined as the number of cars passing a fixed point of the road in a given amount of time or, equivalently, as the product of the density by the velocity: $f = \rho u$.

The LWR model is obtained from the postulate of conservation of vehicles, which yields to the nonlinear partial differential equation

$$\partial_t \rho + \partial_x f = 0, \quad (1)$$

together with the assumption that the speed is a function of the density, namely

$$u(\rho) = V \psi(\rho) \quad (2)$$

where the positive constant V is the vehicular maximal speed, while the function ψ describes how the attitude of drivers depends on the local traffic speed, so that ψ is a monotone (weakly) decreasing \mathcal{C}^1 -function, i.e. $\psi' < 0$, normalized so that $\psi(0) = 1$ and $\psi(1) = 0$.

Below, we use the usual Greenshields speed–density relation, namely

$$\psi(\rho) = 1 - \frac{\rho}{\rho_{max}} \quad (3)$$

where $V > 0$ is the maximal velocity and the maximal density ρ_{max} is normalized to 1, coherently with its interpretation as occupancy.

2 Multispecies Extension of the LWR Model

For the purpose of distinguishing different traffic participants, we extend the LWR model introduced above obtaining a many–species model, see Benzoni-Gavage and Colombo [2003].

The extension to i populations, with $i \in \mathbb{N}^+$, of the conservation law (1) consists of the following system of PDEs

$$\partial_t \rho_j + \partial_x (\rho_j u_j(\rho)) = 0 \quad j = 1, \dots, i, \quad (4)$$

where $\rho = (\rho_j)_{j=1}^i$ is the vector of the populations' densities. A natural extension of the choice (2) leads to

$$u_j(\rho) = V_j \psi \left(\sum_{j=1}^i \rho_j \right) \quad j = 1, \dots, i, \quad (5)$$

where we assume that the speeds are indexed so that $V_{j'} > V_j$ for $j' < j$. With the choice (3), the system is naturally defined on the simplex

$$\mathcal{S} = \left\{ (\rho_j)_{j=1}^i \mid \rho_j \geq 0 \forall j = 1, \dots, i \text{ and } \sum_{j=1}^i \rho_j \leq 1 \right\}.$$

In this paper we only focus on the two species extension of the LWR model, its peculiarity being that it leads to one umbilic point and to a variety of unexpected features. Nevertheless, we mention that for $i > 2$ there exist more than umbilic points. For example, in a three species case we obtain umbilic lines and planes on the boundary of the set of definition. However, the most interesting properties of the multispecies model (1)–(2)–(3) can already be seen in the two species case.

Setting $i = 2$ in (4)–(5), we obtain the two species model

$$\begin{cases} \partial_t \rho_1 + \partial_x (\rho_1 V_1 \psi(r)) = 0 \\ \partial_t \rho_2 + \partial_x (\rho_2 V_2 \psi(r)) = 0 \end{cases} \quad r = \rho_1 + \rho_2. \quad (6)$$

First of all, we investigate the hyperbolicity of (6). The Jacobian $J(\rho)$ of the system is given by

$$J(\rho) = \begin{pmatrix} V_1(\psi(r) + \rho_1 \psi'(r)) & V_1 \rho_1 \psi'(r) \\ V_2 \rho_2 \psi'(r) & V_2(\psi(r) + \rho_2 \psi'(r)) \end{pmatrix} \quad (7)$$

with characteristic polynomial

$$\pi_\rho(\lambda) = (\beta_1 - \lambda)(\beta_2 - \lambda) - \alpha_1 \alpha_2 \quad \text{where} \quad \begin{aligned} \alpha_i &= V_i \rho_i \psi'(r) \\ \beta_i &= V_i(\psi(r) + \rho_i \psi'(r)) \end{aligned} \quad \text{and } r = \rho_1 + \rho_2. \quad (8)$$

Then, the eigenvalues $\lambda_{1/2}(\rho)$ are found as the roots of π_ρ

$$\lambda_1 = \frac{1}{2} \left[(\beta_1 + \beta_2) - \sqrt{(\beta_1 - \beta_2)^2 + 4\alpha_1 \alpha_2} \right], \quad \text{and} \quad \lambda_2 = \frac{1}{2} \left[(\beta_1 + \beta_2) + \sqrt{(\beta_1 - \beta_2)^2 + 4\alpha_1 \alpha_2} \right].$$

Note that, with the above choice, $\lambda_1 \leq \lambda_2$. Moreover, we see that there is no way to find a velocity function ψ for which the eigenvalues of system (6) are distinct on the whole set \mathcal{S} . The LWR model for two species provides one umbilic point where the eigenvalues are the same and hence at this point the system is not strictly hyperbolic. In the case of the Greenshield's relation (3) we obtain the following theorem about the system's hyperbolicity.

Theorem 1. *System (3)–(6) is strictly hyperbolic in $\mathcal{S} \setminus \{\rho^u\}$. At the umbilic point ρ^u , where*

$$\rho^u = (\rho_1^u, 0) \quad \text{with} \quad \rho_1^u = \frac{V_1 - V_2}{2V_1 - V_2}, \quad (9)$$

the eigenvalues λ_1 and λ_2 coalesce.

We now study the consequences of the existence of this point ρ^u on the well posedness of (6). Another system, where hyperbolicity is not strictly given, is studied by Keyfitz and Kranzer [1979/80] and Liu et al. [2016]. Yet, the model discussed here differs from the Keyfitz–Kranzer model because there the umbilic point lies in the interior of the set of definition. In our case the umbilic point lies on the boundary of the simplex \mathcal{S} . Before we study the Riemann Problem of (6), we state some of its global features.

Mention that for $\rho_2 = 0$ the eigenvalues are linear functions in ρ_1 and coincide at ρ_1^u . Indeed,

$$\lambda_1(\rho_1, 0) = \begin{cases} V_2(1 - \rho_1) & \text{for } \rho_1 < \rho_1^u \\ V_1(1 - 2\rho_1) & \text{for } \rho_1 > \rho_1^u, \end{cases} \quad \lambda_2(\rho_1, 0) = \begin{cases} V_1(1 - 2\rho_1) & \text{for } \rho_1 < \rho_1^u \\ V_2(1 - \rho_1) & \text{for } \rho_1 > \rho_1^u. \end{cases} \quad (10)$$

With the above abbreviations (8), a choice of corresponding eigenvectors is given by

$$\mathbf{v}_1 = \begin{pmatrix} \lambda_1 - \beta_2 - \alpha_1 \\ \lambda_1 - \beta_1 - \alpha_2 \end{pmatrix}, \quad \mathbf{v}_2 = \begin{pmatrix} -\lambda_2 + \beta_2 - \alpha_1 \\ \lambda_2 - \beta_1 + \alpha_2 \end{pmatrix}. \quad (11)$$

Hence, we see that in the umbilic point the following holds.

Lemma 1. *At the umbilic point ρ^u given in (9), the Jacobian matrix (7) is not diagonalizable and, in addition to its eigenvalues, its eigenvectors (11) also coalesce. Hence, for this value there exists no basis of eigenvectors for system (6).*

The next proposition describes the corresponding characteristic fields. For the basic terminology we refer to Serre [1999].

Proposition 1. *In $\mathcal{S} \setminus \{\rho^u\}$, with reference to system (3)–(6), the first characteristic field is genuinely nonlinear; the second characteristic field is linearly degenerate for $\rho_1 + \rho_2 = 1$ and genuinely nonlinear elsewhere.*

For the proof of this statement we refer to Benzoni-Gavage and Colombo [2003]. Note that the standard technique relying on the direct computation of $d\lambda_i \cdot \mathbf{v}_i$ is not immediately of use, here.

We recall the following classical result ensuring the invariance of subsets of \mathbb{R}^2 , see Hoff [1985] for more details.

Proposition 2. *A set with regular boundary is locally invariant under a strictly hyperbolic and genuinely nonlinear system of conservation laws if the domain is convex and the normal to the boundary is a left eigenvector of the system.*

We already know that (6) is not strictly hyperbolic and that along the line $\rho_1 + \rho_2 = 1$ it is linearly degenerate, so that Proposition 2 can not be applied to the simplex \mathcal{S} . Nevertheless, by (7),

$$\begin{aligned} (1, 1) J(\rho_1, \rho_2) &= -(\rho_1 V_1 + \rho_2 V_2) (1, 1) & \rho_1 + \rho_2 &= 1; \rho_1, \rho_2 \in [0, 1]; \\ (1, 0) J(0, \rho_2) &= V_1(1 - \rho_2) (1, 0) & \rho_2 &\in [0, 1]; \\ (0, 1) J(\rho_1, 0) &= V_2(1 - \rho_1) (0, 1) & \rho_1 &\in [0, 1]. \end{aligned} \quad (12)$$

Therefore, the normals to the convex set \mathcal{S} are indeed left eigenvectors of the Jacobian J of (6). Thus, we conjecture that \mathcal{S} is invariant, which implies that for initial data inside \mathcal{S} the solution lies inside \mathcal{S} , too. With the above discussion one can now study the Riemann Problem.

2.1 The Riemann Problem when a Species is Absent

After the examination of general features of the LWR model for two species for the Greenshields velocity function, we investigate its well posedness. As we have already seen, the existence of the umbilic point hinders us from using general existence, uniqueness and invariance theorems about hyperbolic conservation laws. Hence, we start with the discussion of existence for particular Riemann Problems (RP). In the case of $i = 2$ populations, the general (RP) consists of system (6) with initial datum

$$\rho(x, 0) = \begin{cases} \rho^L = (\rho_1^L, \rho_2^L) & \text{for } x < 0 \\ \rho^R = (\rho_1^R, \rho_2^R) & \text{for } x > 0 \end{cases} \quad (13)$$

Since we know that (6) is not strictly hyperbolic, the question is whether the existence of the umbilic point influences the solution to the RP (6)–(13) or not. Note, that if we define system (6) on $\mathcal{S} \setminus \{\rho^u\}$, then it will indeed be strictly hyperbolic and thus the solution to the RP (6)–(13) can be found by following the standard Lax theory Lax [1957]. Moreover, (6) is well posed on all initial data with small variation for all times Bressan [2000]. But if we take the point ρ^u into account, it will not be clear whether the solution to the RP problem is well defined. Nevertheless, we can use the Lax-theory to discover the Lax curves and construct the solution to the RP taking care of what happens near the umbilic point. The algebraic expressions are hard to handle and, to our knowledge, there exists no direct proof of well posedness. But one can examine how the umbilic point affects the solution to the RP for a special case. Hence, consider the situation where the slower species is absent at the beginning, i.e., $\rho_2^L, \rho_2^R = 0$. This yields the RP on the ρ_1 -axis, which is (6) together with (13) which now reads

$$\rho(x, 0) = \begin{cases} \rho^L = (\rho_1^L, 0) & \text{for } x < 0, \\ \rho^R = (\rho_1^R, 0) & \text{for } x > 0. \end{cases} \quad (14)$$

Then, we have to include ρ^u into the discussion since the initial data lies on the same axis as the umbilic point. Given any point ρ in \mathcal{S} , the Lax curves $\mathcal{L}^i(\rho)$ are determined by the integral rarefaction curve of the i -th eigenvector along increasing λ_i together with the Hugoniot shock curves.

As a next step we compute the solutions to the RP (6)–(14). Since the Greenshield's function is concave in each entry, the solution to the RP for one species consists of a shock if $\rho_1^L < \rho_1^R$ and of a rarefaction wave if $\rho_1^L > \rho_1^R$. First, we turn to the discontinuities. The shock curves are described with the help of the Rankine Hugoniot (RH) condition.

Proposition 3. *If the Riemann Problem (6)–(13) is solved by two shocks with middle state ρ , then the Rankine Hugoniot condition*

$$\begin{cases} \sigma(\rho^L - \rho) = \mathbf{f}(\rho^L) - \mathbf{f}(\rho) \\ \gamma(\rho - \rho^R) = \mathbf{f}(\rho) - \mathbf{f}(\rho^R) \end{cases} \quad (15)$$

has to be fulfilled, where $\sigma, \gamma \in \mathbb{R}$ are the shock speeds and $\rho \in \mathcal{S}$.

If ρ belongs to the ρ_1 -axis, i.e. $\rho = (\rho_1, 0)$, we are able to describe the the curves exiting ρ completely. Recall that we call Hugoniot set through the point $\rho^0 \in \mathcal{S}$ the set

$$\mathcal{H}(\rho^0) = \{(\rho_1, \rho_2) \in \mathbb{R}^2, \sigma \in \mathbb{R} \mid (16) \text{ holds}\}$$

where

$$\begin{cases} \rho_1((1 - \rho_1 - \rho_2)V_1 - \sigma) = \rho_1^0((1 - \rho_1^0 - \rho_2^0)V_1 - \sigma) \\ \rho_2((1 - \rho_1 - \rho_2)V_2 - \sigma) = \rho_2^0((1 - \rho_1^0 - \rho_2^0)V_2 - \sigma) \end{cases} \quad (16)$$

and, when nec essary, we distinguish between shocks of the first family (\mathcal{H}^1) and of the second family (\mathcal{H}^2), see Bressan [2000], Dafermos [2016] for more details. Whenever ρ^0 lies along the 1 axis, that is we have $\rho_2^0 = 0$, equation (16) become

$$\begin{cases} \rho_1((1 - \rho_1 - \rho_2)V_1 - \sigma) = \rho_1^0((1 - \rho_1^0)V_1 - \sigma) \\ \rho_2((1 - \rho_1 - \rho_2)V_2 - \sigma) = 0. \end{cases} \quad (17)$$

Proposition 4. For $\rho^0 = (\rho_1^0, 0)$ the Hugoniot curves exiting ρ^0 can be described depending on where ρ_1^0 lies along the ρ_1 -axis.

1. If $\rho_1^0 = 0$, then $\mathcal{H}^2(\rho^0) = \{\rho_2 = 0\}$ and $\mathcal{H}^1(\rho^0) = \{\rho_1 = 0\}$.
2. If $\rho_1^0 < \rho_1^*$, then $\mathcal{H}^2(\rho^0) = \{\rho_2 = 0\}$ and $\mathcal{H}^1(\rho^0)$ is monotone in ρ_1 and exits \mathcal{S} at a point with $\rho_2 = 0$ and $\rho_1 > \rho_1^*$.
3. If $\rho_1^* > \rho_1^0 > \rho_1^*$, then $\mathcal{H}^1(\rho^0) = \{\rho_2 = 0\}$ and $\mathcal{H}^2(\rho^0)$ is monotone in ρ_1 and exits \mathcal{S} at a point with $\rho_2 = 0$ and $0 < \rho_1 < \rho_1^*$.
4. If $\rho_1^0 > \rho_1^*$, then $\mathcal{H}^1(\rho^0) = \{\rho_2 = 0\}$ and $\mathcal{H}^2(\rho^0)$ is monotone in ρ_1 and exits \mathcal{S} at a point with $\rho_1 = 0$ and $0 < \rho_2 < 1$.
5. If $\rho_1^0 = 1$, then $\mathcal{H}^1(\rho^0) = \{\rho_2 = 0\}$ and $\mathcal{H}^2(\rho^0) = \{\rho_1 + \rho_2 = 1\}$.

where $\rho_1^* = 1 - V_2/V_1$.

Proof. Study the Hugoniot set 17. The hyperbolæ are given by

$$\rho_2(\rho_1) = \frac{(\rho_1 - \rho_1^0)((V_1 - V_2)(1 - \rho_1) - \rho_1^0 V_1)}{(V_1 - V_2)\rho_1 + \rho_1^0 V_2}.$$

In Figure (1) (a) one sees a sample of the Hugoniot curves for $V_1 = 1$ and $V_2 = 0.75$.

The next proposition confirms that the Hugoniot curves are tangent to the congestion axis $\rho_1 + \rho_2 = 1$, except at the vertexes $(1, 0)$ and $(0, 1)$.

Proposition 5. Let $\rho^0 \in \mathcal{S}$ with $\rho_1^0 + \rho_2^0 < 1$. Then, the Hugoniot curves exiting ρ^0 intersect the $\{\rho_1 + \rho_2 = 1\}$ -axis only for $\rho_1^0 = 0$ or $\rho_1^0 = 1$.

For the proof we refer to Meltzer [2016].

As a next step, we want to find solutions to the RH condition and see whether there is a solution to the RP (6)–(14) consisting of shocks. From the first line in (15) we get the equations

$$\begin{cases} \sigma(\rho_1^L - \rho_1) = f_1(\rho_1^L, \rho_2^L) - f_1(\rho_1, \rho_2) \\ \sigma(\rho_2^L - \rho_2) = f_2(\rho_1^L, \rho_2^L) - f_2(\rho_1, \rho_2) \end{cases} \\ \Leftrightarrow \begin{cases} \sigma(\rho_1^L - \rho_1) = V_1(\rho_1^L - \rho_1)(1 - \rho_1^L - \rho_1) + V_1\rho_1\rho_2 \\ \sigma\rho_2 = \rho_2V_2(1 - \rho_1 - \rho_2) \end{cases}$$

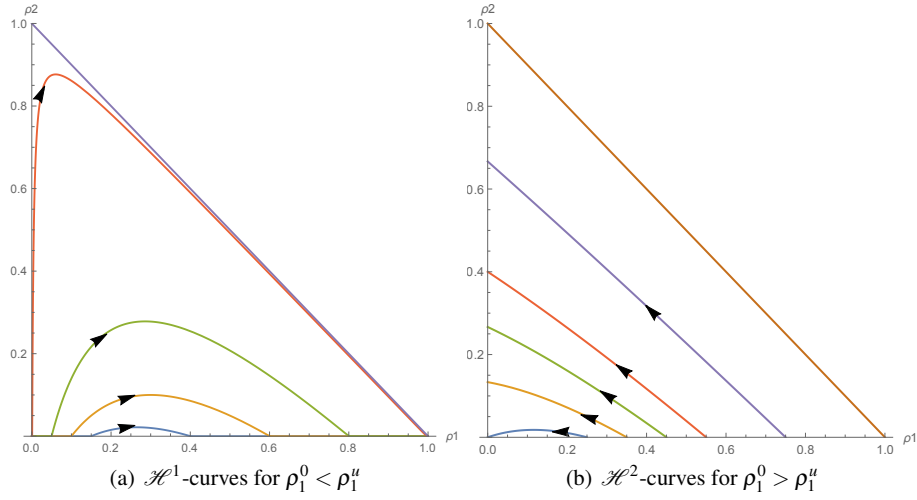


Fig. 1 A sample of \mathcal{H}^1 and \mathcal{H}^2 -curves where $\rho_2^0 = 0$ with $V_1 = 1$ and $V_2 = 0.75$. (The umbilic point is $\rho^u = (0.2, 0)$.)

where a first solution is given by $\rho = (\rho_1^R, 0)$ with the shock speed $\sigma = V_1(1 - \rho_1^R - \rho_1^L)$. The second line of (15) yields

$$\begin{cases} \gamma(\rho_1 - \rho_1^R) = f_1(\rho_1, \rho_2) - f_1(\rho_1^R, \rho_2^R) \\ \gamma(\rho_2 - \rho_2^R) = f_2(\rho_2, \rho_2) - f_2(\rho_1^R, \rho_2^R) \end{cases} \\ \Leftrightarrow \begin{cases} \gamma(\rho_1^R - \rho_1) = V_1(\rho_1^R - \rho_1)(1 - \rho_1^R - \rho_1) + V_1\rho_1\rho_2 \\ \gamma\rho_2 = \rho_2V_2(1 - \rho_1 - \rho_2) \end{cases}$$

A first solution is $\rho = (\rho_1^L, 0)$ with $\gamma = V_1(1 - \rho_1^R - \rho_1^L)$. One obtains that $\sigma = \gamma$. Thus, the solution of only one shock connecting ρ^L and ρ^R may be possible.

From now on $\rho_2 \neq 0$ in (15). Hence, the solution to the Riemann Problem could also consist of two shock curves. The 1-shock curve from ρ^L going to an intermediate state $\rho^m = (\rho_1^m, \rho_2^m) \in \mathcal{S}$ and the 2-shock curve connecting ρ^m with ρ^R . It is necessary that ρ^m is an element of \mathcal{S} . If it lies outside of \mathcal{S} , the solution cannot be constructed by two shock curves. Both shocks have to fulfill the RH condition

$$\begin{cases} \sigma(\rho_1^L - \rho_1^m) = f_1(\rho_1^L, \rho_2^L) - f_1(\rho_1^m, \rho_2^m) \\ \sigma(\rho_2^L - \rho_2^m) = f_2(\rho_1^L, \rho_2^L) - f_2(\rho_1^m, \rho_2^m) \end{cases} \\ \Leftrightarrow \begin{cases} \sigma = V_1(1 - \rho_1^L - \rho_1^m) + V_1 \frac{\rho_1^m \rho_2^m}{\rho_1^L - \rho_1^m} \\ \sigma = V_2(1 - \rho_1^m - \rho_2^m) \end{cases}$$

where $\rho_1^L \neq \rho_1^m$ and

$$\begin{cases} \gamma(\rho_1^m - \rho_1^R) = f_1(\rho_1^m, \rho_2^m) - f_1(\rho_1^R, \rho_2^R) \\ \gamma(\rho_2^m - \rho_2^R) = f_2(\rho_1^m, \rho_2^m) - f_2(\rho_1^R, \rho_2^R) \end{cases} \\ \Leftrightarrow \begin{cases} \gamma = V_1(1 - \rho_1^R - \rho_1^m) + V_1 \frac{\rho_1^m \rho_2^m}{\rho_1^R - \rho_1^m} \\ \gamma = V_2(1 - \rho_1^m - \rho_2^m) \end{cases}$$

where $\rho_1^R \neq \rho_1^m$. Again, $\sigma = \gamma$ and solving for $\rho^m = (\rho_1^m, \rho_2^m)$ yields the intermediate state

$$\begin{aligned}\rho_1^m &= \frac{V_2 \rho_1^L \rho_1^R}{(V_1 - V_2)(1 - \rho_1^L - \rho_1^R)}, \\ \rho_2^m &= - \left[\frac{V_1 - V_2}{V_2} (1 - \rho_1^L - \rho_1^R) - \rho_1^L - \rho_1^R + \frac{V_2 \rho_1^L \rho_1^R}{(V_1 - V_2)(1 - \rho_1^L - \rho_1^R)} \right]\end{aligned}\quad (18)$$

with

$$\begin{aligned}\sigma &= V_2(1 - \rho_1^m - \rho_2^m) \\ &= V_1(1 - \rho_1^L - \rho_1^R)\end{aligned}\quad (19)$$

and $V_1 \neq V_2$, $\rho_1^L + \rho_1^R \neq 1$. The solution is given by two shock curves only if the middle state lies inside of \mathcal{S} . We have to check the condition under which this holds.

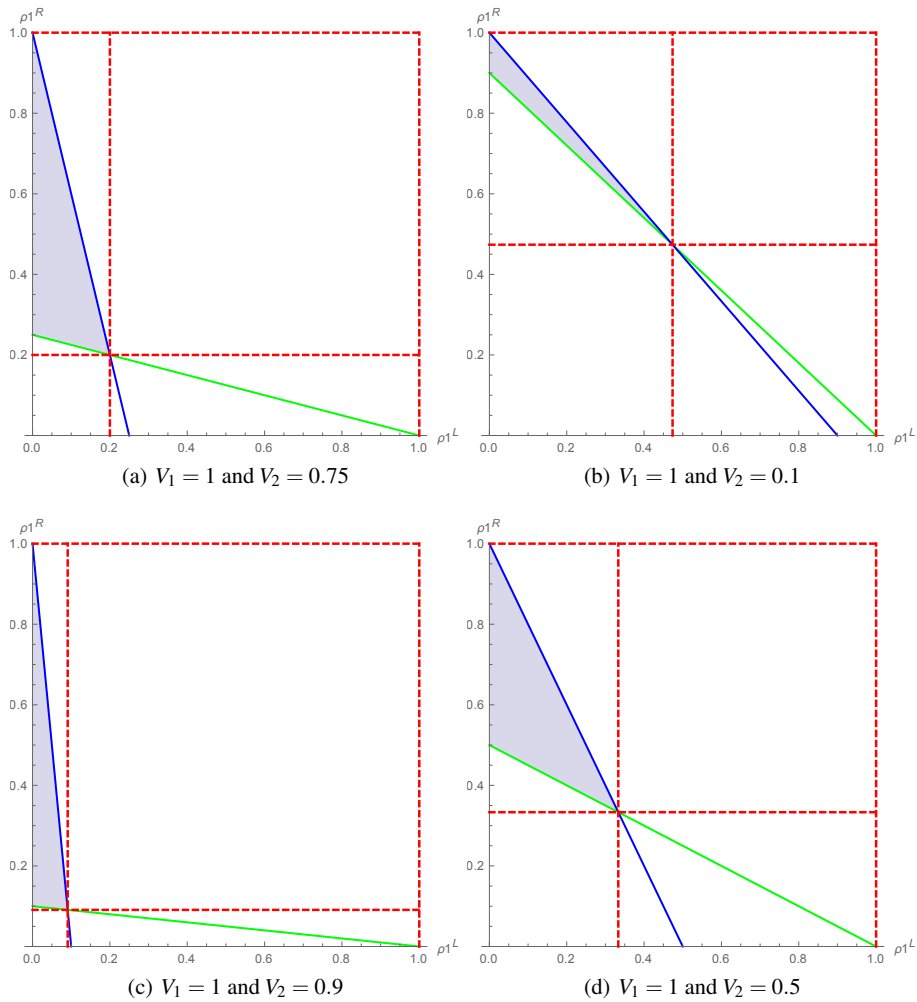


Fig. 2 Values of initial data ρ_1^L and ρ_1^R ($\rho_2^L = \rho_2^R = 0$) for which condition (20) holds with different maximal velocities. The red lines denote the umbilic point and hence restrict the possible values of the initial data. The blue and green line are the values where equality holds in (20). Altogether, corollary 1 is fulfilled in the blue shaded region. Note that, different from the other plots, we are in the ρ_1^L - ρ_1^R -plane.

Corollary 1. For $\rho_1^L < \rho_1^u < \rho_1^R$ the intermediate state ρ^m with coordinates (18) lies in the interior of the simplex \mathcal{S} and hence, the solution to the RP with data $(\rho_1^L, 0)$ and $(\rho_1^R, 0)$ consists of two intersecting shock curves, if

$$\begin{aligned} \frac{V_1}{V_1 - V_2} \rho_1^L + \rho_1^R &\leq 1, \\ \rho_1^L + \frac{V_1}{V_1 - V_2} \rho_1^R &\geq 1. \end{aligned} \tag{20}$$

for $V_1 \neq V_2$.

Proof. It is clear that ρ^m lies inside \mathcal{S} if $\rho_1^m + \rho_2^m \leq 1$ and if $\rho_1^m, \rho_2^m > 0$. Hence, by checking these conditions one obtains (20).

The second condition is needed because for $\rho_1^R < \frac{V_1 - V_2}{V_1}$ the curves of the second family exit the simplex \mathcal{S} on the ρ_1 -axis and not the ρ_2 -axis and hence may intersect with the curves of the first family on the axis, i.e., on the boundary and not in the interior of \mathcal{S} . Then, the middle state (18) does not lie in the interior, either.

The set of values where (20) holds can be seen in Figure 2 for different maximal velocities. The blue and green lines denote the values of ρ_1^L and ρ_1^R where equality holds in (20). The shaded region is the set of values where the inequalities are fulfilled. Altogether, we can state the following.

Proposition 6. *For a RP with $\rho_1^L < \rho_1^u < \rho_1^R$ and $\rho_2^L = \rho_2^R = 0$ the Rankine Hugoniot condition (15) yields two solutions. The first consists of one shock with speed $\sigma = V_1(1 - \rho_1^L - \rho_1^R)$ connecting ρ^L to ρ^R . The second solution contains one shock going from ρ^L to an intermediate state ρ^m and one from ρ^m to ρ^R with the same speed σ . The coordinates of the middle state are*

$$\begin{aligned} \rho_1^m &= \frac{V_2 \rho_1^L \rho_1^R}{(V_1 - V_2)(1 - \rho_1^L - \rho_1^R)} \\ \rho_2^m &= -\frac{V_1 - V_2}{V_2} (1 - \rho_1^L - \rho_1^R) + (\rho_1^L + \rho_1^R) - \frac{V_2 \rho_1^L \rho_1^R}{(V_1 - V_2)(1 - \rho_1^L - \rho_1^R)}. \end{aligned} \tag{21}$$

The second solution is restricted to initial data where ρ^m fulfills (20).

Depending on the position of ρ_1^L on the ρ_1 -axis, the Hugoniot curves yield

1. $\rho_1^L < \rho_1^u$: then $S_2(\rho_1^L, 0) = \{\rho_2 = 0\}$ and $S_1(\rho_1^L, 0)$ is monotone in ρ_1
2. $\rho_1^L > \rho_1^u$: then $S_1(\rho_1^L, 0) = \{\rho_2 = 0\}$ and $S_2(\rho_1^L, 0)$ is monotone in ρ_1

Since $\rho^R = (\rho_1^R, 0)$, it follows that for

1. $\rho_1^L < \rho_1^R < \rho_1^u$ the solution consists only of $S_2 = \{\rho_2 = 0\}$, for
2. $\rho_1^u < \rho_1^L < \rho_1^R$ the solution consists of $S_1 = \{\rho_2 = 0\}$ and for
3. $\rho_1^L < \rho_1^u < \rho_1^R$ the solution consists either only of S_1 or of S_1 and S_2 , intersecting at (21).

Note, that due to the behavior of the Hugoniot curves the solution consists either of one or two intersecting shock curves, depending on the initial data. If both values of the RP lie left or right of the umbilic point, we immediately get the same result as for the one species model. Here, the consistency with the LWR model for one species is given.

As a next step, it is interesting to see how the intermediate state computed from the RH behaves depending on the initial data. For this, we consider some special cases of RP. We start with values close to the umbilic point and examine ρ^m .

Corollary 2. *If the initial data is given by $\rho_1^L = \rho_1^u - \varepsilon$ and $\rho_1^R = \rho_1^u + \varepsilon$ with $\varepsilon > 0$, the intermediate state has the coordinates*

$$\begin{aligned} \rho_1^m &= \rho_1^u - \frac{\varepsilon^2}{\rho_1^u} \\ \rho_2^m &= \frac{\varepsilon^2}{\rho_1^u}. \end{aligned} \tag{22}$$

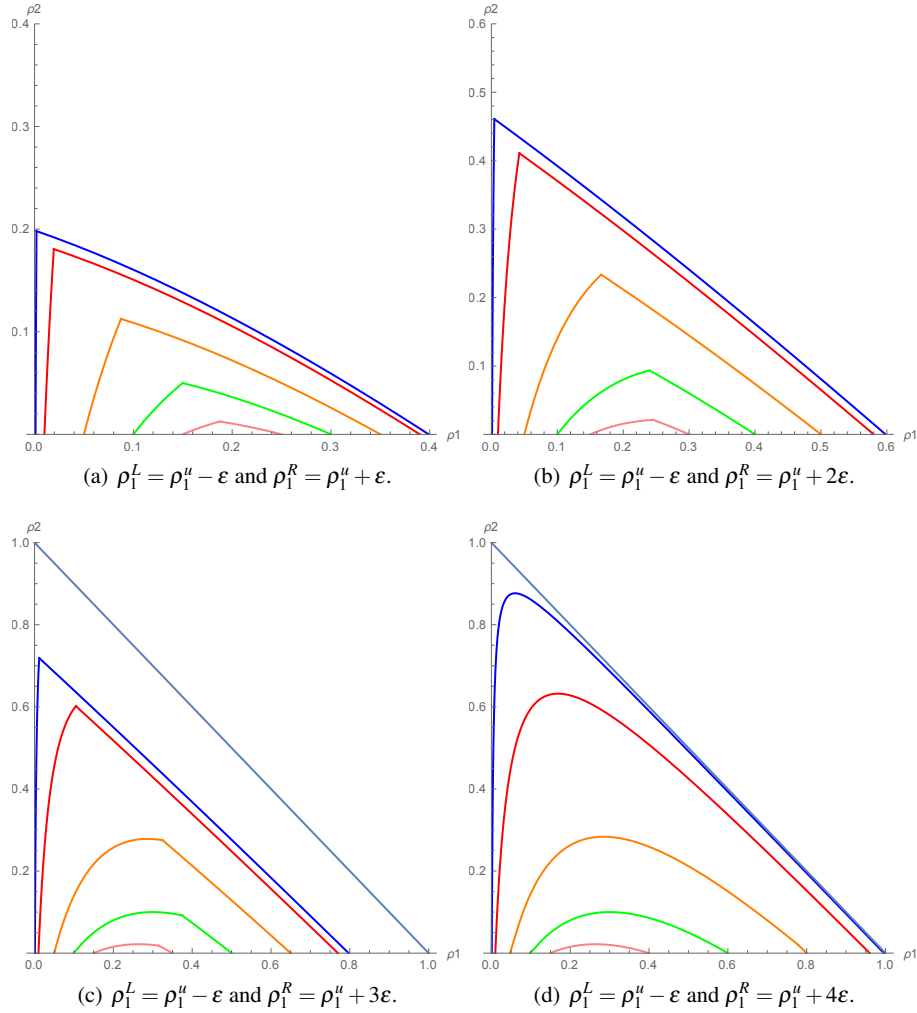


Fig. 3 Sample of intersecting Hugoniot curves for $V_1 = 1$ and $V_2 = 0.75$ and different initial data on the ρ_1 -axis. In the first three pictures, the solution consists of two shock waves intersecting in the interior of \mathcal{S} while in the last one, the solution is given by one curve connecting ρ^L to ρ^R .

Then, one immediately sees that $\varepsilon \rightarrow 0$ yields $\rho^m = \rho^u$. This is convenient since then both initial data equal ρ^u . Now, if ε becomes bigger, the initial data lies more apart of the umbilic point and ρ^m wanders to smaller ρ_1 and bigger ρ_2 . This goes on until $\varepsilon = \rho_1^u$ and thus $\rho_1^L = 0$. At this point, we have

$$\begin{aligned} \rho_1^L &= 0 \\ \rho_1^R &= 2\rho_1^u \end{aligned} \quad (23)$$

and $\rho^m = (0, \rho_1^u)$. Here, the shock speed does not depend on ρ_1^L and ρ_1^R

$$\sigma = V_1(1 - 2\rho_1^u) = V_2(1 - \rho_1^u) \quad (24)$$

and is always positive since $\rho_1^u < 1/2$. Moreover, here the intermediate state lies in the interior of the simplex \mathcal{S} which is consistent with proposition 1 because the initial data fulfills (20). The described behavior can be seen in Figure 3 where we also consider RP with initial data changing in a different relation to each other.

In Figure 3 (b) we see the intersecting Hugoniot curves for initial data with $\rho_1^L = \rho_1^u - \varepsilon$ and $\rho_1^R = \rho_1^u + 2\varepsilon$. This means that the distance between the umbilic point and the right initial datum ρ_1^R grows two times faster than the one between ρ_1^u and ρ_1^L .

In the other two plots in Figure 3 (c) and (d) we see the same with 3ε and 4ε . In (d) we only see one curve because here the equality of condition (20) holds. This implies that for these data there is one shock curve connecting ρ_1^L to ρ_1^R . For data which does not fulfill (20) we have already seen that the solution consists of only one shock curve. We conclude the continuous dependence of the intermediate state from the initial data. Another special case is to start with initial data with nearly maximal distance in \mathcal{S} . This means that ρ_1^L is nearly 0 or ρ_1^R is nearly 1.

Corollary 3. *Consider the RP with $\rho_1^L = 0$ and $\rho_1^R = 1 - \varepsilon$ with $\varepsilon > 0$. The coordinates of the middle state are*

$$\begin{aligned}\rho_1^m &= 0 \\ \rho_2^m &= 1 - \varepsilon \left(1 - \frac{V_1 - V_2}{V_2} \right).\end{aligned}\tag{25}$$

Hence, ρ^m lies on the ρ_2 -axis and moves downward for bigger ε . The shock speed is given by

$$\sigma = \varepsilon V_1.\tag{26}$$

We observe that for $\varepsilon \rightarrow 0$ the middle state equals $\rho^m = (0, 1)$.

Altogether, we described the intermediate state for all values of ρ_1^L and ρ_1^R , respectively. There is continuity between Corollary 2 and Corollary 3. Mention, that the solution consists of two shocks with speed $\sigma = V_1(1 - \rho_1^L - \rho_1^R)$ for both shocks. Hence, the solution does not attain the value ρ^m . For all initial data with $\rho_2^L = \rho_2^R = 0$ the solution to the two species LWR model is given by $\rho(x, t) = (\rho_1(x, t), 0)$ with

$$\rho_1(x, 0) = \begin{cases} \rho_1^L & \text{for } x < \sigma t \\ \rho_1^R & \text{for } x > \sigma t \end{cases}.\tag{27}$$

But before, one must check which of the solutions of Proposition 6 is admissible and to which family the Hugoniot curves belong. For this purpose, the Lax condition must be checked.

Lemma 2. *A shock of the i -th family, connecting ρ^L to ρ^R with speed σ , is admissible in the sense of Lax [1957], if*

$$\lambda_i(\rho^R) \leq \sigma \leq \lambda_i(\rho^L)\tag{28}$$

holds.

If both initial data lie either left or right of the umbilic point, the solution will consist of only one shock. Checking the Lax inequality leads to

1. for $\rho_1^L < \rho_1^R < \rho_1^u$ the condition $\lambda_2(\rho_1^R, 0) < \sigma < \lambda_2(\rho_1^L, 0)$ holds
2. for $\rho_1^u < \rho_1^L < \rho_1^R$ the condition $\lambda_1(\rho_1^R, 0) < \sigma < \lambda_1(\rho_1^L, 0)$ holds.

For $\rho_1^L < \rho_1^u < \rho_1^R$ we have the same shock speed for both shocks and thus the Lax inequality (28) is checked for only one shock from ρ^L to ρ^R . The Lax admissibility conditions are

$$\begin{aligned}\lambda_1(\rho_1^R, 0) &< \sigma < \lambda_1(\rho_1^L, 0), \\ \lambda_2(\rho_1^R, 0) &< \sigma < \lambda_2(\rho_1^L, 0).\end{aligned}\tag{29}$$

with shock speed σ . The eigenvalues yield

$$\begin{aligned}\lambda_1(\rho_1^L, 0) &= V_2(1 - \rho_1^L), \\ \lambda_1(\rho_1^R, 0) &= V_1(1 - 2\rho_1^R), \\ \lambda_2(\rho_1^L, 0) &= V_1(1 - 2\rho_1^L), \\ \lambda_2(\rho_1^R, 0) &= V_2(1 - \rho_1^R).\end{aligned}\tag{30}$$

Hence, we get the next proposition.

Proposition 7. *The Lax admissibility demands that for $\rho_1^L < \rho_1^u < \rho_1^R$ the shock connecting ρ^L to ρ^R with speed σ is*

- a 1-shock if $\rho_1^R > \phi(\rho_1^L)$ and $\phi(\rho_1^R) < \rho_1^L$
- a 2-shock if $\rho_1^R < \phi(\rho_1^L)$ and $\phi(\rho_1^R) > \rho_1^L$
- an over compressive shock if $\rho_1^R < \phi(\rho_1^L)$ and $\phi(\rho_1^R) < \rho_1^L$

with the \mathcal{C}^1 -function

$$\phi(\rho_1) = \frac{(1 - \rho_1)V_1 - V_2}{V_1 - V_2}. \quad (31)$$

with $V_1 \neq V_2$.

Proof. From the expressions (30) one sees that

$$\begin{aligned} \lambda_1(\rho_1^R, 0) &< \sigma \\ \lambda_2(\rho_1^L, 0) &> \sigma. \end{aligned} \quad (32)$$

The other inequalities are obtained by computation

$$\begin{aligned} \sigma < \lambda_1(\rho_1^L) &\Leftrightarrow \phi(\rho_1^R) < \rho_1^L \\ \sigma > \lambda_2(\rho_1^R) &\Leftrightarrow \phi(\rho_1^L) > \rho_1^R. \end{aligned} \quad (33)$$

We observe that the existence of the umbilic point leads to overcompressive shocks. This is also discussed in Benzoni-Gavage and Colombo [2003]. Since we closed the case $\rho_1^L < \rho_1^R$ we now propose that $\rho_1^L > \rho_1^R$.

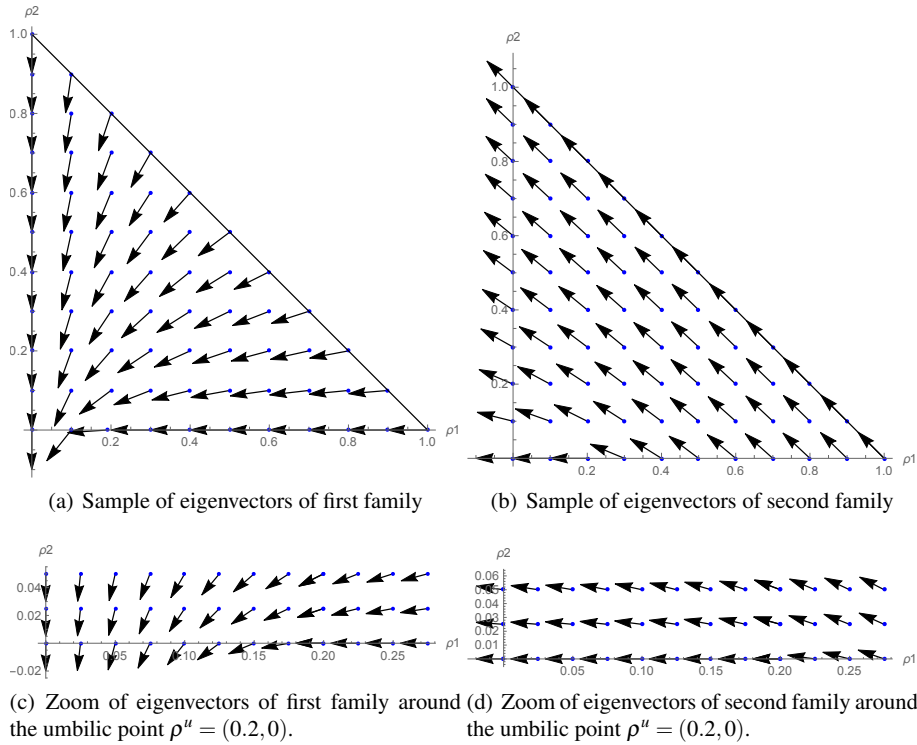


Fig. 4 Sample of eigenvectors with $V_1 = 1$ and $V_2 = 0.75$, oriented so that $d\lambda_i \cdot \mathbf{v}_i > 0$.

By Dafermos [2016], the solution to a single PDE consists of a rarefaction wave. Since we are in the

case of the second species absent, we can use this. The question is, whether the existence of the umbilic point affects the solution similarly to the previous discussed shock waves or not. The rarefaction waves are obtained by integration along the eigenvectors.

A sample of eigenvectors can be seen in Figure 4, oriented so that $d\lambda_i \cdot \mathbf{v}_i > 0$ for $i = 1, 2$. Note that from Theorem 1 both characteristic fields are genuinely nonlinear for data on the ρ_1 -axis. One has already stated in Lemma 1 that the eigenvectors coalesce in the umbilic point, too. We observe this in Figure 4. On the ρ_1 -axis the first eigenvector is parallel to the axis for $\rho_1 > \rho_1^u$ while the second one is parallel for $\rho_1 < \rho_1^u$. In the umbilic point (for the plots $\rho_1^u = 0.2$) they coincide. Moreover, the eigenvectors change continuously with the densities as can be seen in the zoom in Figure 4 (c) and (d). We do not integrate the curves explicitly here, because of the complexity of the algebraic expressions of the eigenvectors. But we are able to compute the eigenvectors on the ρ_1 -axis from equation (11) by using $\rho_2 = 0$. Due to the behavior of the eigenvalues in (10) we also have to make a distinction for the eigenvectors.

$$\mathbf{v}_1(\rho_1, 0) = \begin{cases} \begin{pmatrix} -V_1\rho_1 \\ V_2(1-\rho_1) - V_1(1-2\rho_1) \end{pmatrix} & \text{for } \rho_1 < \rho_1^u \\ \begin{pmatrix} V_1(1-3\rho_1) - V_2(1-\rho_1) \\ 0 \end{pmatrix} & \text{for } \rho_1 > \rho_1^u \end{cases} \quad (34)$$

$$\mathbf{v}_2(\rho_1, 0) = \begin{cases} \begin{pmatrix} -V_1(1-2\rho_1) + V_2(1-\rho_1) \\ 0 \end{pmatrix} & \text{for } \rho_1 < \rho_1^u \\ \begin{pmatrix} -V_1\rho_1 \\ -V_1(1-2\rho_1) + V_2(1-\rho_1) \end{pmatrix} & \text{for } \rho_1 > \rho_1^u \end{cases} \quad (35)$$

We have already seen that in the umbilic point the eigenvectors coalesce.

$$\mathbf{v}_1(\rho_1^u, 0) = \mathbf{v}_2(\rho_1^u, 0) = \begin{pmatrix} -V_1\rho_1^u \\ 0 \end{pmatrix} \quad (36)$$

For $\rho_1^u < \rho_1^L$ the rarefaction wave of the first family passing through ρ_1^L is given by $\mathcal{R}_1(\rho_1^L, 0) = \{\rho_2 = 0\}$. If $\rho_1^R < \rho_1^u$ the 2-rarefaction wave is also described by $\mathcal{R}_2(\rho_1^R, 0) = \{\rho_2 = 0\}$. Hence, for $\rho_1^R < \rho_1^u < \rho_1^L$ and $\rho_2^R = \rho_2^L = 0$ the solution consists of two rarefaction waves with intermediate state $\rho^m = (\rho_1^u, 0)$. Thereby, $\mathcal{R}_1(\rho_1^L, 0)$ goes from ρ^L to ρ^m and $\mathcal{R}_2(\rho_1^R, 0)$ connects the middle state with ρ^R . The solution consists of only one rarefaction curve in the case that both initial data lie left (second family) or right (first family) of the umbilic point. This is consistent with Figure 4 and is the only admissible solution in the sense of Lax [1957]. The two rarefaction curves are equal to each other and so the solution to the RP for the fast species ($\rho_2^L = \rho_2^R = 0$) for the LWR model of two species can again be constructed with the help of the standard LWR model. In the same way as for the shock curves we get $\rho(x, t) = (\rho_1(x, t), 0)$, with

$$\rho_1(x, t) = \begin{cases} \rho_1^L & \text{for } \frac{x}{t} < V_1(1-2\rho_1^L) \\ \frac{1}{2}\left(1 - \frac{x}{Vt}\right) & \text{for } V_1(1-2\rho_1^L) < \frac{x}{t} < V(1-2\rho_1^R) \\ \rho_1^R & \text{for } \frac{x}{t} > V(1-2\rho_1^R) \end{cases} \quad (37)$$

Again, we do not see the middle state because the solution does not attain this value. The existence of the umbilic point does not affect the solution to the RP for rarefaction waves, either.

Closing this subsection, one has to mention that the existence of the solution to the general RP (6)–(14) was not fully proved due to the fact that the expressions of eigenvalues, eigenvectors and shock curves are hard to handle.

2.2 Perturbation of the Riemann Problem

We now want to see whether the solution depends continuously on the initial data or not. Therefore, one can look at a small perturbation $\varepsilon > 0$ of the Riemann Problem (6)–(14) which is (6) together with

$$\rho(x,0) = \begin{cases} \rho^L = (\rho_1^L, \varepsilon) & \text{for } x < 0 \\ \rho^R = (\rho_1^R, \varepsilon) & \text{for } x > 0 \end{cases} \quad (38)$$

We assume that there is a small number of vehicles of the slower species on the road, too. Now we want to examine how this small perturbation of the initial data affects the solution. We again examine the discontinuities and rarefaction waves. Two shocks with speeds σ and γ , connecting ρ^L to ρ^m and ρ^m to ρ^R , have to fulfill the RH condition

$$\begin{cases} \sigma(\rho_1^L - \rho_1^m) = f_1(\rho_1^L, \rho_2^L) - f_1(\rho_1^m, \rho_2^m) \\ \sigma(\rho_2^L - \rho_2^m) = f_2(\rho_1^L, \rho_2^L) - f_2(\rho_1^m, \rho_2^m) \end{cases} \quad (39)$$

$$\Leftrightarrow \begin{cases} \sigma = V_1(1 - \rho_1^L - \rho_1^m) + V_1 \frac{\rho_1^m \rho_2^m - \varepsilon \rho_1^L}{\rho_1^L - \rho_1^m} \\ \sigma = V_2(1 - \varepsilon - \rho_2^m) + V_2 \frac{\rho_1^m \rho_2^m - \varepsilon \rho_1^L}{\varepsilon - \rho_2^m} \end{cases}$$

$$\begin{cases} \gamma(\rho_1^m - \rho_1^R) = f_1(\rho_1^m, \rho_2^m) - f_1(\rho_1^R, \rho_2^R) \\ \gamma(\rho_2^m - \rho_2^R) = f_2(\rho_1^m, \rho_2^m) - f_2(\rho_1^R, \rho_2^R) \end{cases} \quad (40)$$

$$\Leftrightarrow \begin{cases} \gamma = V_1(1 - \rho_1^R - \rho_1^m) + V_1 \frac{\rho_1^m \rho_2^m - \varepsilon \rho_1^R}{\rho_1^R - \rho_1^m} \\ \gamma = V_2(1 - \varepsilon - \rho_2^m) + V_2 \frac{\rho_1^m \rho_2^m - \varepsilon \rho_1^R}{\varepsilon - \rho_2^m} \end{cases}$$

Then, the two shock speeds are not equal. They differ by

$$\gamma - \sigma = V_2 \varepsilon \frac{\rho_1^R - \rho_1^L}{\rho_2^m - \varepsilon}. \quad (41)$$

One observes that the speed of the 2-shock is always greater than the speed of the 1-shock. For $\varepsilon \rightarrow 0$ the speeds are the same again and equal to the shock speed of the unperturbed system. Here, different from the RP ρ_1 -axis, the middle state appears in the solution. This is convenient because the second species is present in this case. Now, the intermediate state ρ^m cannot be computed explicitly from (39) and (40) and thus the exact shock speeds cannot be found either. We can only solve equation (39) and (40) by inserting data for the RP. Moreover, the solution could consist of both, shocks and rarefactions because we are not in a one species case anymore.

By plotting the Hugoniot curves in Figure 5, one sees that the Hugoniot curves depend continuously on the initial data. For data close to the ρ_1 -axis the behavior of the curves changes only slightly. The rarefaction curves are again obtained by integrating along the eigenvectors (4). We get solutions different from the previous case, too, because the eigenvectors are not parallel to the $\{\rho_2 = 0\}$ -axis for data lying in the interior of \mathcal{S} .

2.3 Conclusion

In this contribution we have considered the Riemann problem for the two species extension of the Lighthill Whitam traffic model given by Benzoni-Gavage and Colombo [2003]. We found a solution to the RP for

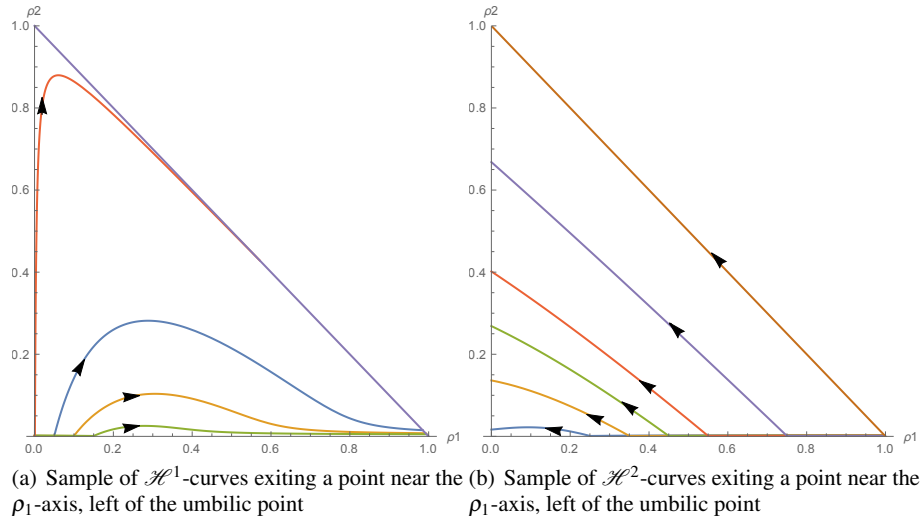


Fig. 5 Sample of Hugoniot curves exiting a point near the ρ_1 -axis with the umbilic point ($\rho^u = (0.2, 0)$) where $V_1 = 1$ and $V_2 = 0.75$.

data on the $\{\rho_2 = 0\}$ -axis. We have seen that the solution depends continuously on the initial data, because if we perturb the RP on the fast axis by $\varepsilon > 0$, small, we will observe a small variation in the Lax curves.

The general RP is defined in (6) – (13) for the LWR model for two species. The complexity of the

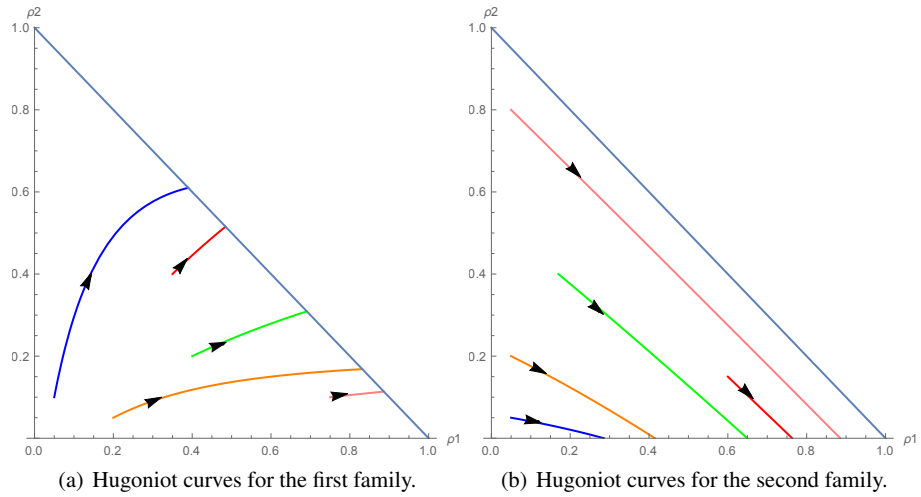


Fig. 6 Sample of Hugoniot curves with $V_1 = 1$ and $V_2 = 0.75$ for initial data lying in the interior of \mathcal{S} .

expressions hinders us from further general search for explicit expressions related to system (6). We know that for initial data with small variation different from the umbilic point, the RP is well posed. But for a general RP with data lying far apart, it is difficult to prove well posedness due to the complexity of the expressions. The idea is to find a middle state ρ^m as the intersection of the two Lax curves $\mathcal{L}^1(\rho^L)$ and $\mathcal{L}^2(\rho^R)$. Mention that now the solution can also contain both shocks and rarefaction waves and on the $\{\rho_1 + \rho_2\}$ -axis contact discontinuities.

In Figure 6 one sees samples of shock curves belonging to the first and second family. The rarefaction waves are obtained by integrating along the eigenvectors, which have already been plotted in Figure 4. These plots give no indication that the RP (6) should be ill posed, as was conjectured in by Benzoni-Gavage

and Colombo [2003]. For data different from the umbilic point, the system is indeed strictly hyperbolic and around ρ^u we solved the RP. Moreover, the simplex \mathcal{S} is convex and because of (12) we assume its invariance. But since we have no (global) proof of well posedness for all initial data, we cannot be sure that the lack of global strict hyperbolicity does not lead to ill posedness.

To summarize, the extension of the LWR model to a two populations model proves to be difficult, since global hyperbolicity is not given. There exists an umbilic point on the boundary of the set where we define the system, meaning at the boundary the eigenvalues coalesce. To the best of our knowledge well-posedness of a similar model (w. umbilic point on the boundary) has *not* been discussed in the literature. Moreover, the model, although it is of simple structure, yields intricate expressions for the corresponding eigenvalues and vectors. Even though our studies seem to hint at well-posedness of this model, a proof of well-posedness of our model seems elusive.

References

- S. Benzoni-Gavage and R. M. Colombo. An n -populations model for traffic flow. *European J. Appl. Math.*, 14(5):587–612, 2003. ISSN 0956-7925. doi: 10.1017/S0956792503005266. URL <http://dx.doi.org/10.1017/S0956792503005266>.
- A. Bressan. *Hyperbolic systems of conservation laws*, volume 20 of *Oxford Lecture Series in Mathematics and its Applications*. Oxford University Press, Oxford, 2000. ISBN 0-19-850700-3. The one-dimensional Cauchy problem.
- C. M. Dafermos. *Hyperbolic conservation laws in continuum physics*, volume 325 of *Grundlehren der Mathematischen Wissenschaften [Fundamental Principles of Mathematical Sciences]*. Springer-Verlag, Berlin, fourth edition, 2016. ISBN 978-3-642-04047-4. doi: 10.1007/978-3-642-04048-1. URL <http://dx.doi.org/10.1007/978-3-662-49451-6>.
- D. Hoff. Invariant regions for systems of conservation laws. *Trans. Amer. Math. Soc.*, 289(2):591–610, 1985. ISSN 0002-9947. doi: 10.2307/2000254. URL <http://dx.doi.org/10.2307/2000254>.
- B. L. Keyfitz and H. C. Kranzer. A system of nonstrictly hyperbolic conservation laws arising in elasticity theory. *Arch. Rational Mech. Anal.*, 72(3):219–241, 1979/80. ISSN 0003-9527. doi: 10.1007/BF00281590. URL <http://dx.doi.org/10.1007/BF00281590>.
- P. D. Lax. Hyperbolic systems of conservation laws. II. *Comm. Pure Appl. Math.*, 10:537–566, 1957. ISSN 0010-3640.
- M. J. Lighthill and G. B. Whitham. On kinematic waves. II. A theory of traffic flow on long crowded roads. *Proc. Roy. Soc. London. Ser. A.*, 229:317–345, 1955. ISSN 0962-8444.
- S. Liu, F. Chen, and Z. Wang. Existence of global L^p solutions to a symmetric system of Keyfitz–Kranzer type. *Appl. Math. Lett.*, 52:96–101, 2016. ISSN 0893-9659. doi: 10.1016/j.aml.2015.08.011. URL <http://dx.doi.org/10.1016/j.aml.2015.08.011>.
- M.-C. Meltzer. Multispecies traffic models based on the Lighthill-Whitham and the Aw-Rascle model. *Thesis*, 2016. URL https://www.mathematik.uni-wuerzburg.de/~klingen/Workgroup_files/Thesis_Marie-Christine_Meltzer.pdf.
- P. I. Richards. Shock waves on the highway. *Operations Res.*, 4:42–51, 1956. ISSN 0030-364X.
- D. Serre. *Systems of conservation laws. 1*. Cambridge University Press, Cambridge, 1999. ISBN 0-521-58233-4. doi: 10.1017/CBO9780511612374. URL <http://dx.doi.org/10.1017/CBO9780511612374>. Hyperbolicity, entropies, shock waves, Translated from the 1996 French original by I. N. Sneddon.